PERGAMON

Organic Geochemistry 33 (2002) 877–895

Organic Geochemistry

www.elsevier.com/locate/orggeochem

Sulfur speciation in kerogens of the Orbagnoux deposit (Upper Kimmeridgian, Jura) by XANES spectroscopy and pyrolysis

Géraldine Sarret[a], Thierry Mongenot[b], Jacques Connan[c], Sylvie Derenne[b], Masoud Kasrai[a], G. Michael Bancroft[a], Claude Largeau[b,*]

[a]*Chemistry Department, University of Western Ontario, London, Ontario, Canada N6A 5B7*
[b]*Laboratoire de Chimie Bioorganique et Organique Physique, UMR CNRS 7573, ENSCP, 11 rue Pierre et Marie Curie, 75231 Paris Cedex 05, France*
[c]*Elf Exploration Production, CSTJF, 64018 Pau Cedex, France*

Received 8 May 2000; accepted 31 May 2002
(returned to author for revision 17 September 2000)

Abstract

Thermally immature, extremely sulfur-rich kerogens from the Orbagnoux deposit have been extensively studied over the last few years for their chemical structure, source organisms and depositional conditions. However, important uncertainties remain concerning sulfur speciation in these kerogens and changes in sulfur functionality that occur upon thermal stress. In the present study sulfur speciation for isolated kerogens from the five facies recognized in the deposit was established via K- and L-edge X-ray Absorption Near Edge Structure (XANES) spectroscopy. A representative sample of the most organic-rich facies of the deposit, the dark parallel laminae, was examined by "direct" pyrolysis at 400 °C and the results compared with those previously derived from "indirect" pyrolysis (carried out under the same conditions but from kerogen pre-heated at 300 °C). XANES examination was performed on the unheated kerogen, the pre-heated kerogen, the insoluble pyrolysis residues and the effluents obtained via these two pyrolyses. Sulphur distribution was also determined via elemental analyses and measurements of evolved H_2S. Identification of the pyrolysis products of the "direct" experiment was performed by gas chromatographic/mass spectrometric analyses, before and after desulfurization, of the crude pyrolysate and of separated fractions and sub-fractions. Substantial quantitative and qualitative differences are thus noted between the "direct" and "indirect" pyrolyses at 400 °C, as a result of the cleavage and aromatization of some sulfide bridges occurring upon pre-heating at 300 °C. Thus, the "indirect" pyrolysis appears somewhat less efficient for the thermal cracking of the macromolecular structure of the kerogen. Nevertheless, it provides more detailed information on the intermolecularly sulfur-linked carbon skeletons that build up the bulk of this structure owing to (i) the release of OSC with higher carbon numbers and (ii) the much easier desulfurization of the molecular aggregates probably due to a lower degree of cross-linking. XANES spectroscopy showed that (i) thiophenes are the main sulfur species in the unheated kerogens and (ii) substantial aromatization of the non-thiophenic sulfur forms occurs upon the thermal treatments.

1. Introduction

The Orbagnoux deposit (Upper Kimmeridgian, Southern Jura Mountains, France) is characterized by conspicuous accumulations of oil-prone, thermally immature, and extremely sulfur-rich organic matter (OM). This deposit has been mined for over a century

* Corresponding author. Tel.: +33-1-4329-5102; fax: +33-1-4325-7975.
E-mail address: clargeau@ext.jussieu.fr (C. Largeau).

0146-6380/02/$ - see front matter
PII: S0146-6380(02)00066-9

for producing sulfur-rich shale oils used to prepare pharmaceutical and cosmetic products (e.g. Koch et al., 1985; Czarnetzki, 1986). Sulfur contents of up to 17.5 wt.% were observed for isolated kerogens from the Orbagnoux section (Mongenot et al., 1997, 2000). Several previous studies dealt with depositional conditions during the formation of this remarkable deposit formed in a lagoonal setting on a shallow carbonate platform (Gubler and Louis, 1956; Bernier and Courtinat, 1979; Bernier, 1984; Gorin et al., 1989; Tribovillard et al., 1991, 1992; Mongenot et al., 1997, 2000; van Kaam-Peters and Sinninghe Damsté, 1997; van Kaam-Peters et al., 1998). Extensive studies were also focused on the chemical structure of the kerogen, source organisms and formation pathway (van Kaam-Peters et al., 1995, 1998; Koopmans et al., 1996; van Kaam-Peters and Sinninghe Damsté, 1997; Mongenot et al., 1997, 1999). The five carbonate facies recognized in the deposit were thus shown to originate from the development of cyanobacterial mats (light undulated laminae), coccolith blooms (massive limestones), and the interaction between cyanobacterial activity and coccolith settling (dark undulated laminae, dark or light parallel laminae). It also appeared that the so-called natural sulfurization pathway played a major role in OM preservation for all of these facies.

The dark parallel laminae facies, abundantly occurring in the Orbagnoux deposit, exhibits especially high TOC values. In a recent study (Mongenot et al., 1999) the kerogen isolated from a representative sample of this facies, termed TM9sa, was examined via a combination of pyrolytic and spectroscopic (FTIR, solid state ^{13}C NMR) methods. "Off-line" pyrolysis on TM9sa kerogen was carried out under the same conditions as previously used for various kerogens (Largeau et al., 1986): the material was first pre-heated at 300 °C for 20 min so as to eliminate volatile compounds possibly adsorbed on the kerogen surface and/or included in the kerogen matrix, and after extraction with organic solvents the pre-heated kerogen was pyrolysed at 400 °C for 1 h. Analyses by gas chromatography–mass spectrometry (GC–MS) of the highly complex pyrolysate thus obtained were focused on the high molecular weight sulfur-containing constituents, which account for the bulk of the crude pyrolysate. Such analyses, carried out both before and after desulfurization of the pyrolysis products using Raney nickel, indicated that the macromolecular structure of TM9sa kerogen is chiefly based on intermolecularly sulfur-linked chains, cross-linked via (poly)sulfide bridges, derived from cyanobacterial and coccolithophorid lipids (Mongenot et al., 1999). However, the GC-amenable constituents of the pyrolysate mostly consisted of a mixture of heterocyclic organic sulfur compounds (OSC) based on thiophene, bithiophene, benzothiophene and dibenzothiophene units. In addition, comparison of the FTIR spectra of kerogen before and after pre-heating at 300 °C showed some changes, including a shift in the C=C stretching vibration from 1635 to 1600 cm^{-1} that likely reflects the occurrence of aromatization reactions during pre-heating. Indeed, it was previously observed that (poly)sulfide bridges in sulfur-rich macromolecules are rapidly cleaved under thermal stress, and that the radicals thus formed can undergo cyclization, yielding thiophene groups (Schmid, 1986; Krein and Aizenshtat, 1994; Cohen et al., 1995; Tomic et al., 1995; Koopmans et al., 1995). Thus, the abundant thiophenic functions detected in the GC-amenable constituents of the TM9sa pyrolysate might correspond, at least in part, to groups generated during the pre-heating and/or during pyrolysis at 400 °C. Moreover, FTIR and solid state ^{13}C NMR spectra did not provide any precise information on sulfur speciation. Thus, there was no evidence either about the occurrence of thiophenic groups in the unheated kerogen or, more generally, about the nature and relative abundance of sulfur-containing functions in this material.

Sulfur speciation in coals, kerogens and recent sediments has been previously studied using various methods, including analytical pyrolysis and chemical degradation (e.g. Calkins, 1987; Kelemen et al., 1991, 1993; Sinninghe Damsté and de Leeuw, 1990; Sinninghe Damsté et al., 1990; Eglinton et al., 1990, 1992), high pressure temperature-programmed reduction (e.g. Mitchell et al., 1994; Brown et al., 1997, 2000) and X-ray Absorption Near Edge Structure (XANES) spectroscopy. In the past, the latter method has been used to study coals (Spiro et al., 1984; Huffman et al., 1989, 1991; Brown et al., 1992; Kasrai et al., 1996a), rock extracts, heavy petroleum asphalts and asphaltenes (George and Gorbaty, 1989; Gorbaty et al., 1990; George et al., 1990; Waldo et al., 1991, 1992; Green et al., 1993; Eglinton et al., 1994; Kasrai et al., 1994; Nelson et al., 1995; Schouten et al., 1995; Sarret et al., 1999a,b), whole sediments (Vairavamurthy et al., 1994, 1995), and kerogens (Eglinton et al., 1994; Nelson et al., 1995, Riboulleau et al., 2000). This spectroscopic method presents several characteristics that make it a useful probe for sulfur speciation in complex natural systems. XANES is element-specific, sensitive to the electronic structure, oxidation state and local symmetry of the absorbing site, is non destructive and does not require any sample pre-treatment that might create artifacts.

The main purposes of the present study were to (i) derive information on sulfur speciation in TM9sa kerogen, (ii) examine the nature and the extent of the changes in sulfur functions induced by pre-heating at 300 °C and to (iii) determine the influence of such changes on the quantitative and qualitative features of the fractions (insoluble pyrolysis residue and trapped pyrolysate) obtained via subsequent pyrolysis at 400 °C. To

this end, additional pyrolysis was carried out by direct heating of TM9sa kerogen at 400 °C and the results of this "direct" experiment were compared with those previously obtained from "indirect" pyrolysis, carried out under the same conditions but following pre-heating at 300 °C. Pyrolysis products were identified via GC/MS analysis of the different fractions separated from the crude pyrolysate by column chromatography (CC) and thin layer chromatography (TLC). GC/MS analyses were also carried out after Raney Ni desulfurization of the crude pyrolysate, the toluene-eluted fraction, and the methanol-eluted non-acid fraction. Information on sulfur functions was obtained via S K- and L-edge XANES spectroscopy. XANES spectra for the raw kerogens, corresponding to seven other samples from the different facies of the Orbagnoux section, were also examined in order to derive general information on sulfur speciation in this especially sulfur-rich deposit. Then, sulfur speciation was studied in the pre-heated TM9sa kerogen and in the insoluble residues and pyrolysates obtained after "direct" and "indirect" pyrolyses at 400 °C (Fig.1).

2. Experimental

2.1. Samples

Samples from the five different facies were picked from the mined section. The thickness of these samples was adjusted (down to a few millimeters in some cases) so as to avoid contamination by the adjacent facies and to obtain "pure" materials in terms of colour and texture. The location, the meaning of the code and the bulk geochemical features of these samples are described in Mongenot et al. (2000). The ground rocks were extracted with $CHCl_3$/MeOH (2/1, v/v) by stirring for 12 h at room temperature, prior to treatment with HF/HCl (Durand and Nicaise, 1980). A second extraction with $CHCl_3$/MeOH was carried out after this acid treatment. Elemental analysis of the kerogens thus isolated showed very low ash contents (e.g. 1.2 wt.% in the case of TM9sa) and X-ray diffraction indicated that residual ash corresponded to fluorides, probably formed during the HF treatment (Mongenot et al., 2000). No significant amounts of pyrite or other sulfur-containing minerals were found in these kerogen concentrates.

2.2. XANES spectroscopy

The XANES experiments were performed at the Canadian Synchrotron Radiation Facility situated on the 1 GeV electron storage ring, Alladin, University of Wisconsin. Experimental details have been described previously (Kasrai et al., 1994). The materials (unheated kerogens, pre-heated kerogen, insoluble pyrolysis residues, crude pyrolysates and pyrolysate fractions dried under vacuum) were ground and the powder was spread onto double-faced carbon tape stuck on a metal holder for the XANES measurement. All the K- and L-edge spectra presented in this paper were recorded using total electron yield detection. S K- and L-edge spectra were background-subtracted using a linear function extrapolated from the pre-edge region. The spectra were then normalized to the height of the maximum of peak B for the L-edge, and to the height of the edge jump for the K-edge. S K- and L-edge spectra were simulated by a linear combination of reference spectra using a least-squares fitting program. Details of the fitting procedure are given in Tables 1 and 2.

For the S K-edge analysis, previous examination of a large database of model compounds showed that the precision is good for the oxidized species (sulfoxides, sulfones, sulfonic acids, sulfates) but weaker for the reduced ones (alkyl sulfides, aryl sulfides and thiophenic sulfides) because the area of the main peak used for the quantification of the species varies significantly from one compound to another within a given family and because energy shifts between the three families are small (Sarret et al., 1999b). For this reason, we chose to consider alkyl sulfides, aryl sulfides and thiophenic sulfides as a whole (termed "sulfides + thiophenes" in Table 1). Similarly, alkyl and aryl sulfides were combined in the XANES study of asphalts by Green et al. (1993). In contrast, disulfides can be distinguished from sulfides as their peak is shifted by 1–2 eV.

For S L-edge spectra the energy shift between the different sulfide species is larger, and the energy resolution better (0.2 eV compared to 1.0 eV for the K-edge) (Fig. 2). These characteristics make it possible to distinguish disulfides, alkyl sulfides, aryl sulfides and thiophenes (Kasrai et al., 1994, 1996a,b; Sarret et al., 1999a,b). No alkylarylsulfide reference was used in the present study so this sulfur form, which probably occurs in kerogens, could not be considered in the data analysis. In contrast, peaks corresponding to the most oxidized species (sulfones, sulfonic acids, and sulfates) are badly resolved, and difficult to analyze quantitatively (Sarret et al., 1999a,b). Thus sulfoxides were the only oxidized species quantified from L-edge spectra.

K- and L-edge spectra are therefore complementary for the quantification of the following species: disulfides, "sulfides + thiophenes", sulfoxides, sulfones, sulfonic acids, and sulfates for the K-edge; disulfides, alkyl sulfides, aryl sulfides, thiophenic sulfides, and sulfoxides for the L-edge. Hence, the agreement of K- and L-edge results can be tested on the disulfide and sulfoxide contents.

For each K- and L-edge simulation, all the model compounds of our database were tested. The error, estimated as the differences in obtained proportions

Table 1
Relative proportions (%) of sulfur species in the raw kerogens and pyrolysis products determined by simulating their S K-edge XANES spectra[a]

Sample	FM	Reduced S (%)		Oxidized S (%)			
		Disulfides	"Sulfides + thiophenes"	Sulfoxides	Sulfones	Sulfonates	Sulfates
Unheated kerogens							
TM15 (massive limestone)	0.08	16	78	3	0	0	3
TM14 (dark undulated laminae)	0.06	18	77	3	0	0	2
TM12 (dark undulated laminae)	0.09	18	77	3	0	0	2
TM11 (light parallel laminae)	0.08	16	78	3	0	0	3
TM9sb (dark parallel laminae)	0.07	14	82	2	0	0	2
TM9sa (dark parallel laminae)	**0.06**	**22**	**73**	**2**	**0**	**3**	**0**
TM8b (light parallel laminae)	0.08	18	76	4	0	2	0
TM5 (light undulated laminae)	0.13	27	68	0	0	4	1
Pyrolysis products of TM9sa kerogen							
"Indirect" pyrolysis							
Pre-heated kerogen	0.05	18	78	0	0	1	3
Insoluble pyrolysis residue	0.08	0	92	3	0	0	5
Trapped pyrolysate[b]	0.06	0	95	5	0	0	0
Toluene fraction	0.06	0	94	6	0	0	0
Methanol fraction	0.03	0	86	12	0	0	2
"Direct" pyrolysis							
Insoluble pyrolysis residue	0.08	0	90	4	0	0	6
Trapped pyrolysate	0.04	0	97	3	0	0	0
Toluene fraction	0.04	0	94	6	0	0	0

[a] The spectra were simulated by a linear combination of reference spectra shown in Sarret et al. (1999b) using a least-squares fitting program. The figure of merit of the fit is defined as $FM = \Sigma(f_{experimental} - f_{fit})^2$ in the 2468–2485 eV range.

[b] Only negligible amounts of trapped products were recovered upon pre-heating at 300 °C so that the trapped material analysed for the "indirect" experiments corresponded to the one obtained at 400 °C.

Table 2
Relative proportions (%) of reduced sulfur species and sulfoxides in the raw kerogens and pyrolysis products determined by simulating their S L-edge XANES spectra[a]

Sample	FM	Disulfides	Aryl sulfides	Alkyl sulfides/thiols	Thiophenes	Sulfoxides
Unheated kerogens						
TM15	0.3	8	0	22	70	0
TM12	0.5	15	0	26	59	0
TM11	0.7	10	0	25	65	0
TM9sa	**1.5**	**12**	**0**	**22**	**66**	**0**
TM8b	1.6	11	0	24	65	0
TM5	0.5	12	0	31	57	0
Pyrolysis products of TM9sa kerogen						
Pre-heated kerogen	0.2	0	0	25	70	5
Insoluble residue of "indirect" pyrolysis	1.3	0	0	0	50	50
Insoluble residue of "direct" pyrolysis	0.3	0	0	0	70	30
Pyrolysis effluents	0.3–0.6	0	0	10–20	65–70	10–20

[a] See note (a) Table 1. The figure of merit of the fit is defined in the 162–168 eV range.

between two fits of equivalent quality, was ±10% (absolute percentage) for both edges. As an illustration, Fig. 2f compares two simulations of comparable quality, as measured by the figure of merit of the fits (FM defined in Note a, Table 1), that differ in the nature of the thiophene model compound used.

2.3. "Direct" pyrolysis of TM9sa kerogen

The analytical flow chart for the "direct" pyrolysis of TM9sa kerogen is shown in Fig. 1. "Off-line" pyrolysis was performed as previously described (Largeau et al., 1986) under a helium flow (40 ml/min). The kerogen (ca. 1 g) was directly pyrolysed at 400 °C for 1 h. and pyrolysis products were trapped in $CHCl_3$ at −5 °C. The crude pyrolysate was separated by CC on alumina (40 g: activity 2) into three fractions by eluting with heptane (440 ml), toluene (160 ml) and methanol (160 ml), respectively. The heptane-eluted fraction was further separated by TLC (developed with heptane/diethyl ether: 95/5) into six subfractions. The methanol-eluted fraction was separated into non-acid and acid constituents by NaOH/HCl extraction.

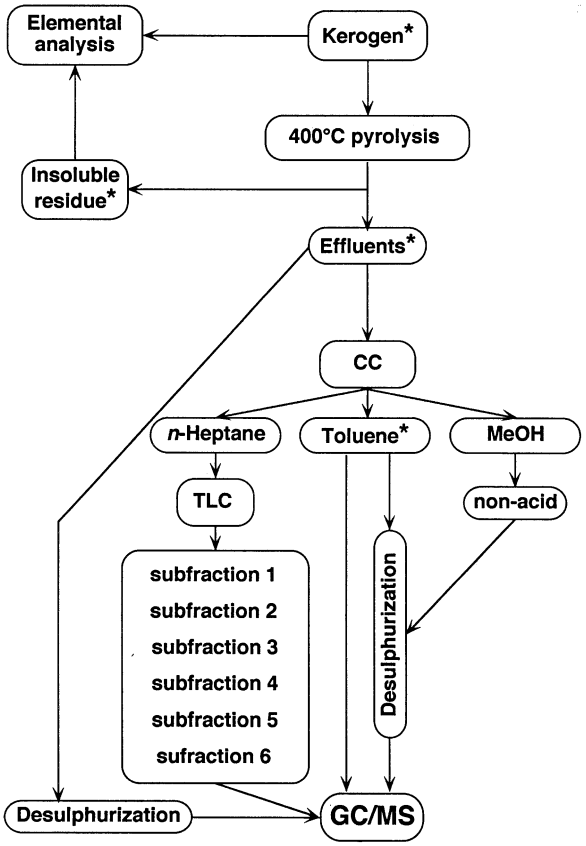

Fig. 1. Analytical flow chart for the study of TM9sa kerogen by "direct" pyrolysis at 400 °C. *Samples examined by XANES spectroscopy.

2.4. Raney nickel desulfurization and hydrogenation

Desulfurization was carried out according to Sinninghe Damsté et al. (1988a) on the crude pyrolysate,

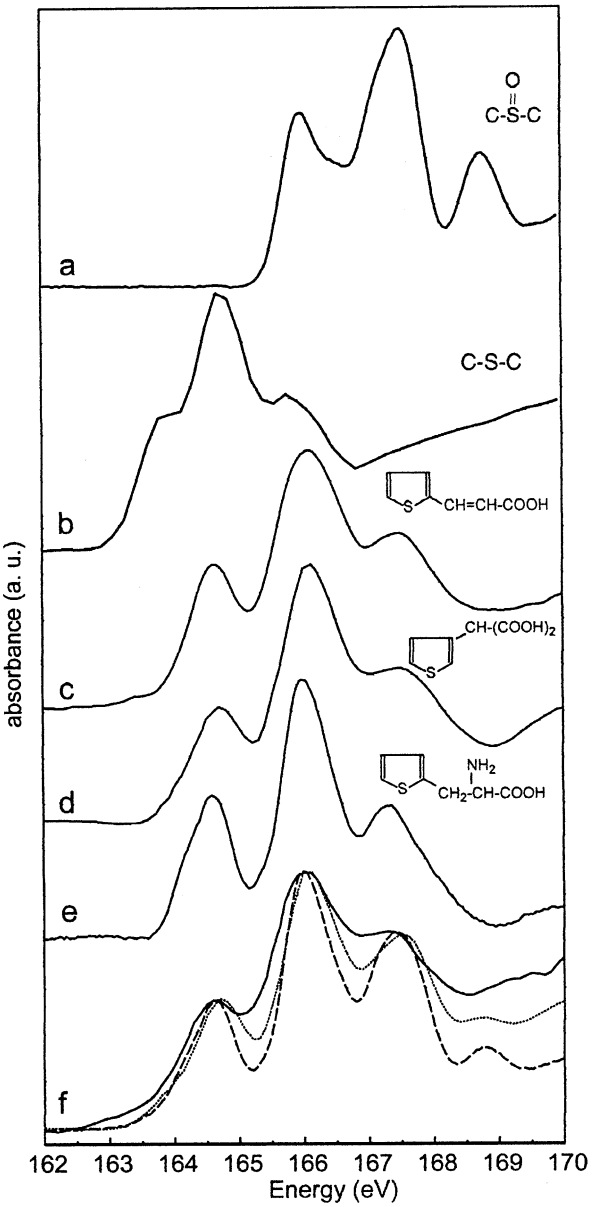

Fig. 2. S L-edge XANES spectra for DL-methionine sulfoxide (a), DL-methionine (b), 3-(2-thienyl)-DL-acrylic acid (c), 3-thiophene malonic acid (d), 3-(2-thienyl)-DL-alanine (e), and two simulations of a kerogen spectrum (f): dotted line: linear combination of 15% (a) + 21% (b) + 64% (d); dashed line: linear combination of 13% (a) + 34% (b) + 53% (e).

the toluene-eluted fraction and the methanol-eluted non-acid fraction. The dried desulfurized products were dissolved in 5 ml of ethyl acetate; 5 mg of PtO_2 (Aldrich), two drops of acetic acid were added and hydrogen was bubbled through the solution for 1 h. Acid and reduced platinum were removed on a Na_2SO_4/Na_2CO_3 (1 g/1 g) column eluted with ethyl acetate (50 ml).

2.5. GC/MS

GC/MS was carried out on a Hewlett-Packard 5890 gas chromatograph interfaced to a 5989A Hewlett-Packard mass spectrometer operated at 70 eV with a mass range m/z 40–600. The gas chromatograph was equipped with a 25 m CPSil 5 CB (film thickness: 0.4 μm) column. Helium was the carrier gas. The oven was heated from 100 to 300 °C at 4 °C min^{-1}. Identifications of the OSC were based on comparison with reference compounds and/or elution orders of previously described compounds (Sinninghe Damsté et al., 1986, 1988a,b; Mongenot et al., 1999).

2.6. Sulfur distribution

This distribution was detemined for ''direct'' and ''indirect'' pyrolyses via (i) measurement of sulfur contents in pyrolysates and pyrolysis residues by elemental analysis and (ii) gravimetrical determination of H_2S by passing the pyrolysis effluents into a 10 wt.% $AgNO_3$ basic solution.

3. Results and discussion

3.1. XANES spectroscopy

3.1.1. Unheated kerogens

S K-edge XANES spectra for the eight kerogen samples are compared in Fig. 3. The distribution of sulfur species was determined by simulating each spectrum by a linear combination of reference spectra, as shown for TM15 kerogen (Fig. 3b). Table 1 shows that for all the facies, the major sulfur moieties are ''sulfides + thiophenes'' (68–82% of total sulfur). Disulfides account for 14–27% of total sulfur, and some oxidized species probably occur in low amounts. The disulfide fraction may contain some other types of polysulfides (trisulfides,...) as the main peak occurs at about the same energy as disulfides (Chauvistré et al., 1997).

S L-edge XANES spectra for the Orbagnoux kerogens are compared to spectra for some reference compounds in Fig. 4. The kerogen spectra exhibit three peaks labeled A, B and C at about the same energy position as the thiophene reference compound. However, the peak A/peak B intensity ratio for the kerogens is higher than for the thiophene reference (0.84–0.93 compared to 0.56), and peak A shows a shoulder between 163.0 and 163.5 eV. These features probably reflect the presence of minor species. The kerogen spectra were simulated by linear combinations of reference spectra, including one thiophene compound plus one or two other type of model compounds, as exemplified for TM9sa kerogen in Fig. 5. Poor quality fit was obtained with the aryl sulfide reference, as its peak B energy corresponds to the valley between peaks A and B for the kerogen (CL4 in Figs. 4 and 5). Thus, this species is either absent from the kerogen, or present in small amount. The kerogen spectrum was best reproduced by linear combinations of thiophene as the major S species (66%), thiol and disulfide (22 and 12%, respectively) (Table 2, Fig. 5). As thiol and alkyl sulfide spectra are similar, a fit of equivalent quality was obtained by replacing the thiol by an alkyl sulfide reference. Similar distributions were obtained from the S L-edge spectra for the other Orbagnoux kerogens.

K- and L-edge results were consistent, with a difference in the proportion of disulfides between 3 and 15% (Tables 1 and 2). Therefore, it is concluded that thiophenes are the major sulfur species in kerogens for the five facies of the Orbagnoux deposit and that less abundant species include disulfides, alkyl sulfides and/or thiols. Some oxidized species probably occur in low amounts. The thiophenic entities are probably linked to some alkyl chains or condensed with other aromatics in the kerogen macromolecules, but sulfur XANES spectroscopy is not sensitive to substituents on the thiophenic ring. In this paper the term ''thiophene'' refers to any thiophenic unit whatever its substituents.

A S K-edge XANES study previously showed that polysulfides constituted the major part of the organic sulfur in recent sediments from offshore Chile (Vairavamurthy et al., 1995). Kerogens, isolated from sulfur-rich recent sediments off the Peru margin (considered as modern precursors of type II-S kerogens) and from thermally immature sulfur-rich sediment of the Monterey Formation, California), were also previously examined using this spectroscopic method (Eglinton et al., 1994; Nelson et al., 1995).S K-edge spectra pointed to a predominant contribution of acyclic sulfides, and a relatively low content of thiophenes (ca. 20–30 wt.% of total sulfur) in these kerogens. However, examination of the kerogens from the same set of Peru sediments and of the same type II-S Monterey kerogen by high pressure temperature-programmed reduction (TPR), along with XANES analysis of the generated oils (Brown et al., 1997), showed levels of thiophenic sulfur up to 45% of total sulfur. TPR also revealed a large increase in thiophene with depth, not observed via S K-edge XANES spectroscopy. Similarly, the results obtained in the present study, from K- and L-edge data on kerogens from the Orbagnoux deposit indicate a large contribution of thiophenes in these sulfur-rich immature samples.

3.1.2. Pyrolysis products of TM9sa kerogen

The S K-edge XANES spectra for TM9sa kerogen and heated insoluble materials are compared in Fig. 6a. The spectra for the unheated kerogen and the kerogen pre-heated at 300 °C look similar, but closer examination shows that the main peak for the latter material is slightly shifted to the right (Fig. 6b). Accordingly, the simulations indicate that the relative abundance of disulfides is slightly lower in the pre-heated kerogen than in the unheated sample (18% compared to 22%) whereas

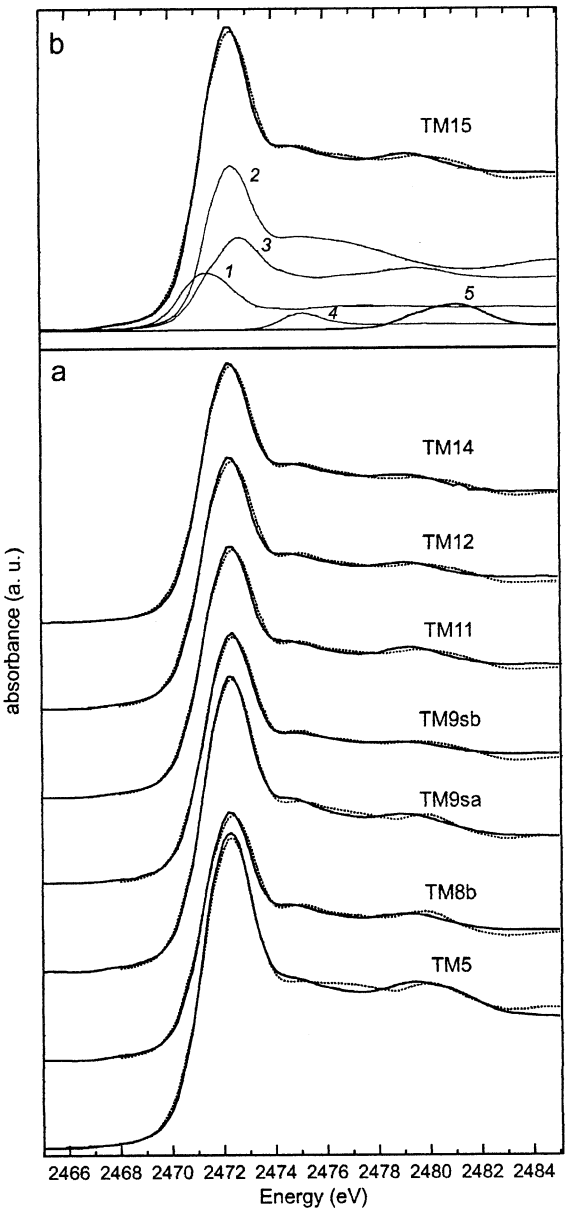

Fig. 3. (a) S K-edge XANES spectra (solid lines) and their simulation (dotted lines) for Orbagnoux kerogens from the different facies (see Table 1); (b) S K-edge XANES spectrum for TM15 kerogen (solid line) and its simulations (dotted line). The best fit consisted of a linear combination of disulfide (dibenzyl disulfide, 1), alkyl sulfide (DL-methionine, 2), thiophene (3-(2-thienyl)-DL-acrylic acid, 3), sulfoxide (DL-methionine sulfoxide, 4) and sulfate (dodecyl sulfate, 5).

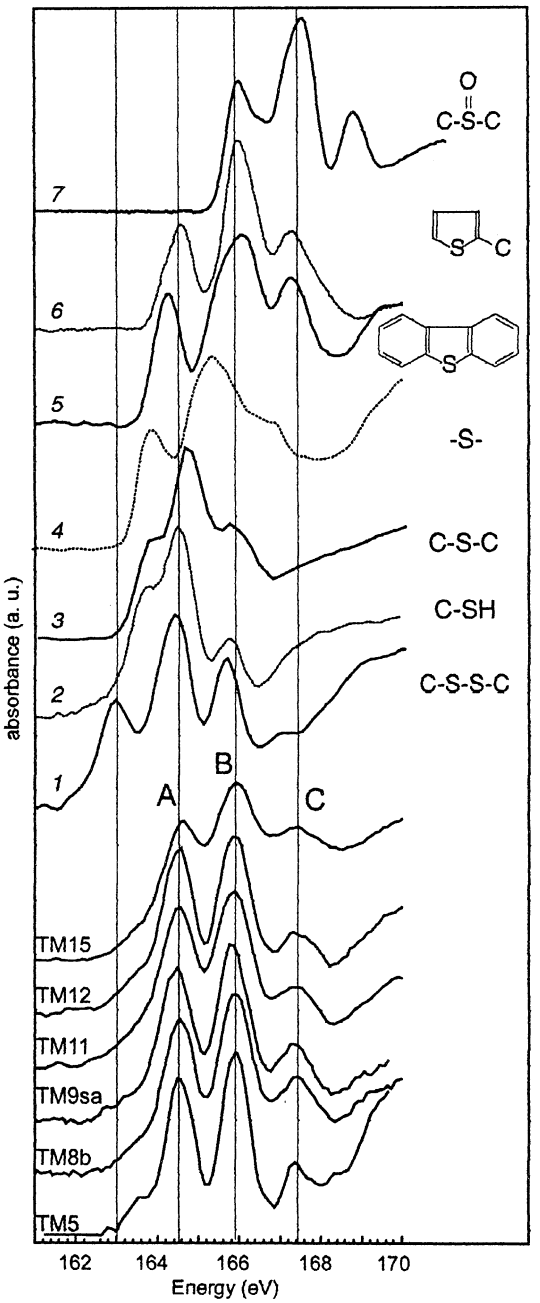

Fig. 4. Comparison of the S L-edge XANES spectra for the Orbagnoux kerogens and for some reference compounds: DL-cystine (1), DL-cysteine (2), DL-methionine (3), poly(phenylene sulfide) (4), dibenzothiophene (5), 3-(2-thienyl)-DL-alanine (6), and DL-methionine sulfoxide (7).

the content of sulfides is substantially higher (78% compared to 73%) (Table 1). The small oscillation at 2475 eV visible on the unheated kerogen spectrum is absent for the pre-heated material (arrows in Fig. 6a), and the oscillation at about 2480 eV is shifted to the right (Fig. 6c). These latter features are consistent with a decrease in the sulfoxide content to negligible levels, and an increase of the amount of more oxidized species, respectively. However, the simulations show that these changes in the proportions of oxidized S species are within the precision of the method (Table 1). For the residues from pyrolyses at 400 °C, a clear shift to the right of the main peak is observed (Fig. 6b).The simulations point to the lack of disulfides in the residues from "direct" and "indirect" pyrolyses whereas very high proportions of "sulfides + thiophenes" are obtained (Table 1). The removal of disulfides upon heating is consistent with the high sensitivity of di(poly)sulfides to thermal stress previously observed by Nelson et al. (1995) using XANES spectroscopy combined with hydrous pyrolyses on a sulfur-rich kerogen from the Monterey Formation. A shift to the right is also observed

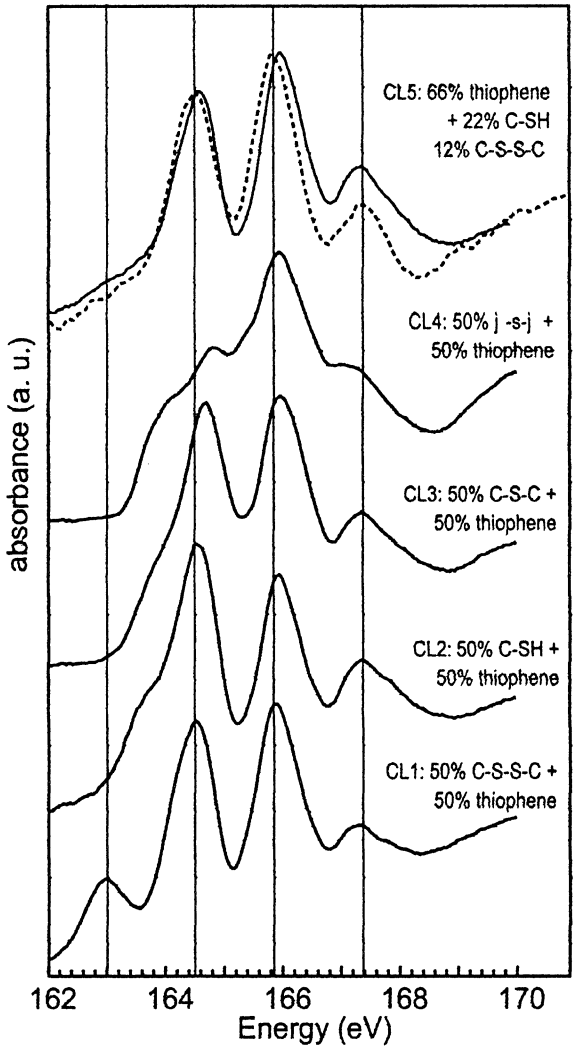

Fig. 5. Comparison of S L-edge XANES spectrum for TM9sa kerogen (dotted line) with linear combinations of spectra 1, 2, 3, 4 and 6 presented in Fig. 4 (solid lines).

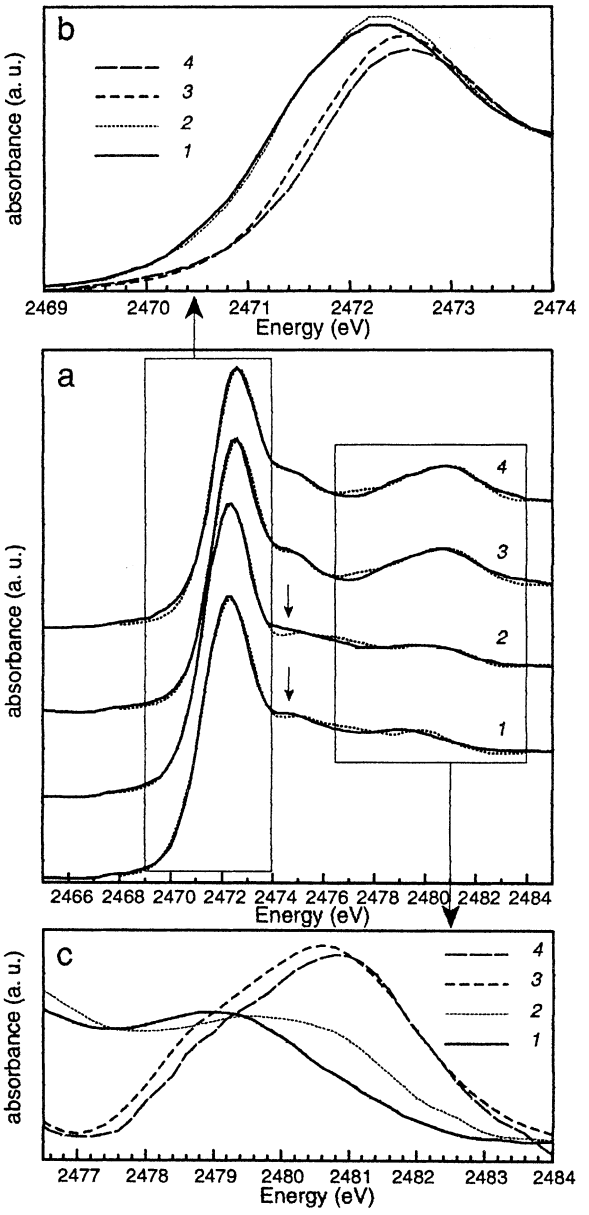

Fig. 6. (a) S K-edge XANES spectra (solid lines) and simulations (dotted lines) for TM9sa unheated kerogen (1), kerogen pre-heated at 300 °C (2), insoluble residue from "indirect" (3) and "direct" (4) pyrolysis at 400 °C. (b, c) Zooms of the experimental spectra in the 2469.0–2474.0 eV (b) and 2476.5–2484.0 eV (c) region.

for the oscillation at 2480 eV in the residues from pyrolyses at 400 °C (Fig. 6c), reflecting an increasing contribution of oxidized sulfur species. Nevertheless, the relative abundances obtained for these species are still within the precision of the method.

The S L-edge spectra for TM9sa kerogen and heated insoluble materials are compared in Fig. 7. A decrease of peak A intensity and increase of peak C intensity is observed going from the unheated kerogen to the 300 and 400 °C residues. For the material pre-heated at 300 °C, the simulations indicated a composition of 70% thiophene, 25% thiol and/or alkyl sulfides and a low level of sulfoxides (Table 2). The spectra of the 400 °C residues were simulated by a mixture of thiophenes (50 and 70% for the "indirect" and "direct" residues, respectively) and sulfoxides (50 and 30%, respectively). Peak C might also contain a contribution of more oxidized species, such as sulfones. Thus, consistent with numerous studies on coal (e.g. Calkins, 1987; Kelemen et al., 1991, 1993), the 400 °C pyrolysis eliminated the acyclic sulfides present in the raw and pre-heated kerogens, and the sulfur retained in the pyrolysis residues is largely thiophenic.

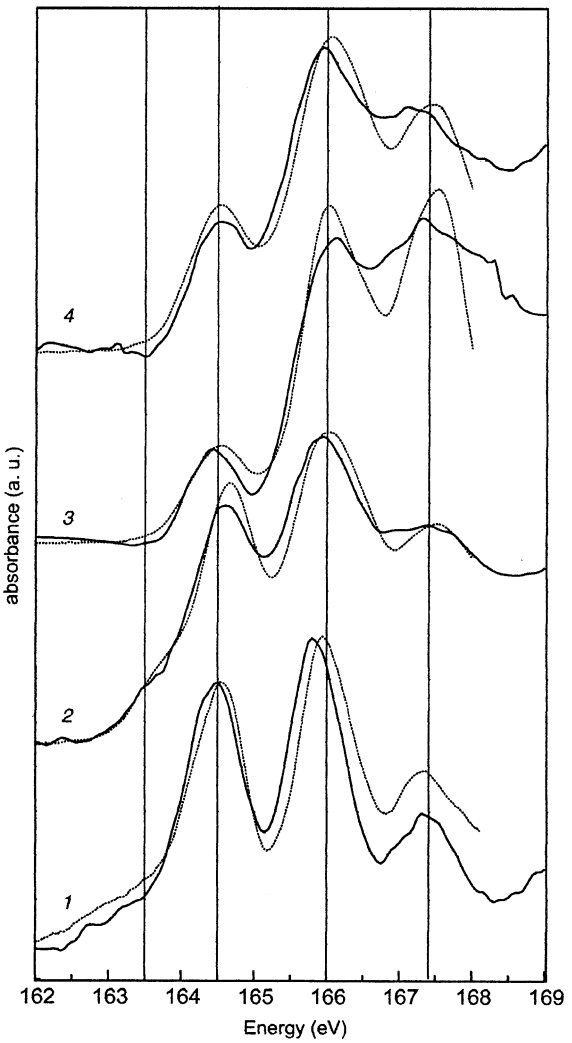

Fig. 7. S L-edge XANES spectra (solid line) and their simulations (dotted lines) for TM9sa unheated kerogen (1), kerogen pre-heated at 300 °C (2), insoluble residue from "indirect" (3) and "direct" (4) pyrolysis at 400 °C. Simulations consist of a combination of spectra 2, 6 and 7 presented in Fig. 4.

The comparison of K- and L-edge results shows that S L-edge spectroscopy underestimates the disulfide content in the pre-heated kerogen, and greatly overestimates the sulfoxide content in the 400 °C residues. As the K- and L-edge results were consistent for the unheated kerogens, we believe that this disagreement is not an artifact. Given that S L-edge spectroscopy, using total electron yield detection, probes only a few tens of nm in depth compared to several hundreds nm for the K-edge (Kasrai et al., 1996b), this indicates that the surface of the grains is much more oxidized than the bulk. Such a feature probably reflects surface oxidation during sample handling, possibly during grinding and the residue of "indirect" pyrolysis appears more oxidized than the "direct" one.

S K-edge spectra for the trapped effluents from "direct" and "indirect" pyrolyses are compared in Fig. 8, and the results of the spectral simulations are presented in Table 1. These pyrolysates are sharply dominated by sulfides (95 and 97% of total sulfur for the "indirect" and "direct" experiments, respectively). Minor amounts of sulfoxides are also observed but the corresponding products were not detected by GC/MS due to their high polarity. As expected, these polar compounds are found in the methanol-eluted fraction and to a lesser extent in the toluene-eluted one. The trapped effluents and toluene fractions from "direct" and "indirect" pyrolyses exhibit similar S K-edge spectra and no substantial difference is detected between the two procedures.

Fig. 9 compares the S L-edge spectra for the trapped effluents and toluene fractions from "direct" and "indirect" pyrolyses. Like the K-edge spectra, they look similar, and their three peak positions match the thiophene reference. Peak A, present as a small shoulder centered at about 163.5 eV, might be due to a limited contribution of alkyl sulfides and/or thiols, and peak C/peak B intensity ratios are higher than for the thiophene reference (0.62–0.82 compared to 0.45), so these effluents likely contain some sulfoxides. The spectra were simulated using a combination of alkyl sulfide and/or thiols (10–20% depending on the spectrum), thiophene (65–70%) and sulfoxide (10–20%) (Table 2, Fig. 9). The proportion of sulfoxide is higher than determined by K-edge analysis. Again, this disagreement is attributed to oxidation of the surface of the samples, which may have occurred during the drying procedure used to

isolate the effluents in a solid form. Substantial oxidation, resulting in the formation of sulfoxides, was observed by Eglinton et al. (1994) in the molecular size fractions of bitumens isolated by preparative gel permeation chromatography from recent marine sediments (Peru upwelling) and rock samples (Monterey Formation).

It is therefore concluded from the K- and L-edge analysis that the effluents from "direct" and "indirect" pyrolyses of TM9sa kerogen contain thiophenes as major sulfur species, and some alkyl sulfides and/or thiols and oxidized moieties as less abundant forms. No significant difference is detected between these effluents by XANES spectroscopy.

3.2. Geochemical data on the "direct" pyrolysis of TM9sa kerogen

The bulk quantitative features of the "direct" pyrolysis at 400 °C are reported in Table 3 and compared with those obtained from the "indirect" experiment. Substantial differences can be noted between these two methods. "Direct" pyrolysis is characterized by (i) a very large production of pyrolysis products (ca. 90 wt.% compared to 85 wt.% for the "indirect" procedure), (ii) a relatively larger production of highly volatile products, although the trapped components dominate in both cases, (iii) a much higher recovery for the three fractions upon column chromatographic separation. Indeed, the high molecular weight sulfur-rich molecular aggregates retained on the column that dominate the pyrolysate for the "indirect" experiment (Mongenot et al., 1999) (ca. 55 wt.%) account for only ca. 19 wt.% of

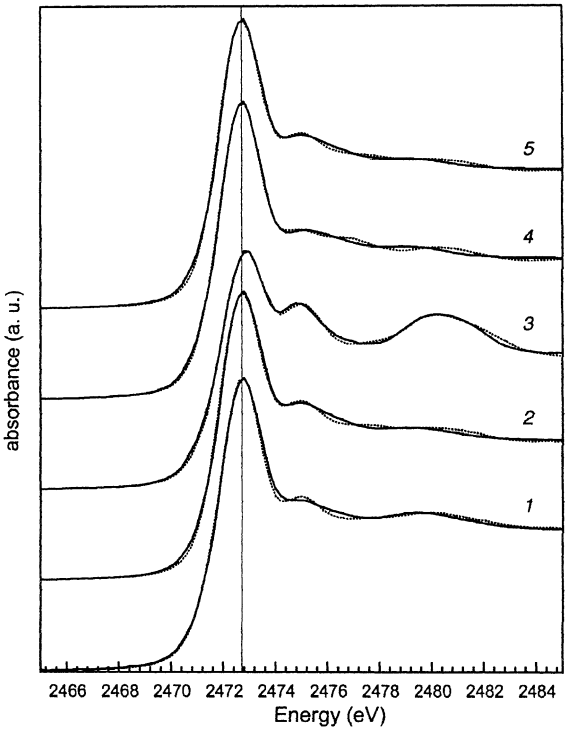

Fig. 8. S K-edge XANES spectra (solid lines) and their simulation (dotted lines) for the crude pyrolysate (1), the toluene-eluted fraction (2) and the methanol-eluted fraction (3) from "indirect" pyrolysis, and for the crude pyrolysate (4), and toluene-eluted fraction (5) of "direct" pyrolysis.

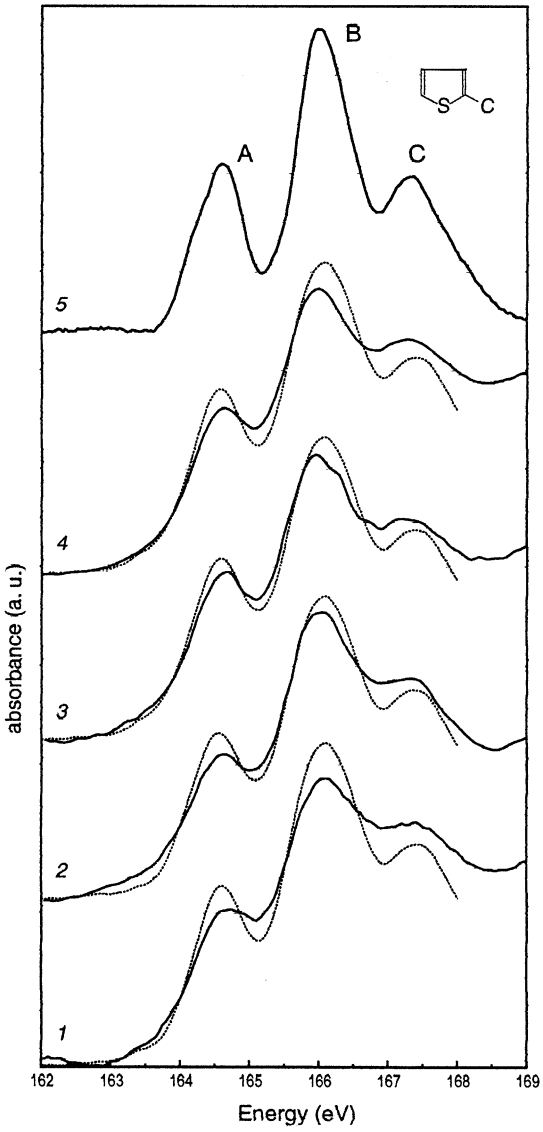

Fig. 9. S L-edge XANES spectra for the crude pyrolysates (1, 3) and toluene-eluted fractions (2, 4) of "indirect" and "direct" pyrolyses, respectively, and for 3-(2-thienyl)-DL-alanine (5). Simulations consist of a combination of spectra 2, 6 and 7 presented in Fig. 4.

the crude pyrolysate for the "direct" procedure. The same decrease in the H/C atomic ratio to 0.75 for the pyrolysis residues, compared to 1.44 in the unheated kerogen, is observed in both cases, thus indicating similar levels of aromatization along with the release of aliphatic moieties. In contrast, different evolution profiles are noted for the S org/C atomic ratio. For the "indirect" procedure, this ratio slightly increases (0.10 compared to 0.09 in the initial kerogen), which may indicate that organic carbon is somewhat more efficiently released than organic sulfur. From the elemental analysis and the abundance of this residue and the elemental analysis of the unheated kerogen, it can be calculated that ca. 14 wt.% of the total sulfur is retained in the "indirect" pyrolysis residue. In contrast, the S org/C atomic ratio decreases upon "direct" pyrolysis (0.07), and only ca. 3 wt.% of the total sulfur is retained in the residue. Thus, sulfur is more efficiently released by this method. Most of the resistant sulfur occurring in both residues is probably located in condensed aromatic structures with a high thermal stability formed upon pyrolysis, as previously observed for various kerogens and coals (Gillaizeau et al., 1997 and references therein). Such condensed structures would correspond to the bulk of the heterocyclic sulfides that account for most of the total sulfur retained in the 400 °C residues by S K-edge and S L-edge XANES spectroscopy. However, the latter method could not distinguish condensed and simple thiophenes.

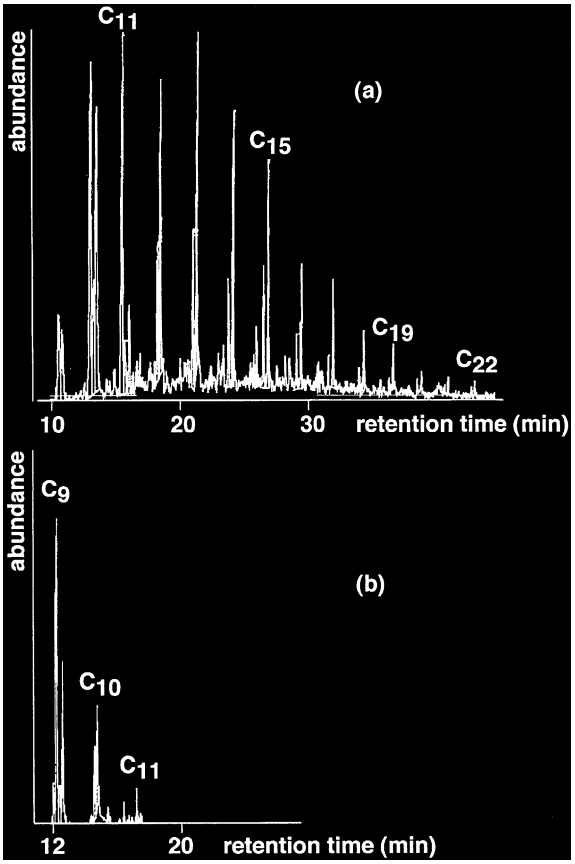

Fig. 10. Comparison of the distributions of the *n*-alkylbenzothiophenes formed upon "indirect" (a) and "direct" (b) pyrolysis of TM9sa kerogen (mass chromatogram *m*/*z* 147).

Taken together, the above features indicate that the thermal cleavage of the macromolecular structure of the TM9sa kerogen is relatively more efficient under "direct" conditions, especially for the release of sulfur-containing functions. It therefore appears that the changes in the chemical structure of the TM9sa kerogen associated with pre-heating at 300 °C, revealed by XANES spectroscopy, partly hinder their release upon subsequent pyrolysis. As stressed in the Introduction, FTIR spectra suggest that such changes are probably associated with aromatization processes. Such processes, classically observed upon kerogen heating (e.g. Rouxhet et al., 1980; Durand and Monin, 1980), also account for the larger amount of insoluble residue obtained via "indirect" pyrolysis (ca. 15 wt.% instead of ca. 10 wt.%).

Aromatization should also be reflected by changes in sulfur distribution between different fractions obtained upon pyrolysis of TM9sa. In fact, the H_2S evolved can be considered to represent the minimal amount of non-thiophenic sulfur that occurs in this kerogen. Sulfur contents in the trapped pyrolysates and pyrolysis residues were therefore determined for the "direct" and "indirect" pyrolyses along with the sulfur released as H_2S. The total amount thus measured accounted for 79 and 84 wt.% of the sulfur in the initial kerogen for the "direct" and "indirect" experiments respectively. The sulfur occurring in the high volatility organic sulphur compounds generated upon heating could not be measured in these "off-line" pyrolyses. The substantial amounts of sulfur not accounted for in the mass balances, 21 and 16 wt.%, respectively, should chiefly correspond to these volatile compounds. The relatively lower recovery observed for the "direct" pyrolysis is consistent with the higher amount of volatile products, relative to the trapped ones, formed under these conditions (Table 3). The H_2S production corresponds to 23 and and 18 wt.% of total sulfur for the "direct" and "indirect" experiments, respectively, whereas XANES spectroscopy indicated a content of non-thiophenic sulphur of ca. 34%. These differences reflect partial aromatization of the non-thiophenic sulphur of the kerogen into thiophenic structures upon pyrolyses. As expected, this aromatization is somewhat more pronounced in the case of the "indirect" experiment, hence lower H_2S release, due to the onset of aromatization during the pre-heating treatment at 300 °C.

3.3. GC–MS results on the "direct" pyrolysis of TM9sa kerogen

Detailed analysis of the composition of the "direct" pyrolysate was performed in the present study for comparison with the "indirect" experiment. Several tens of homologous series of organic sulfur compounds were identified, including thiophenic and sulfidic products, as observed in previous pyrolyses of TM9sa kerogen (van Kaam-Peters and Sinninghe Damsté, 1997, Mongenot et al., 1999). Comparison of the composition of the trapped products of the "direct" and "indirect" pyrolyses revealed a number of common features (not discussed here) but, also, substantial differences. It thus appears that (i) some pyrolysis products identified in the latter case are not generated via "direct" pyrolysis, (ii) the relative abundance or the distribution of some series is markedly modified and (iii) new pyrolysis products are formed through "direct" pyrolysis. Accordingly, the changes in chemical structure due to pre-heating can induce (or preclude) the formation of several series of pyrolysis products upon subsequent heating at 400 °C, and they can also modify the distribution of other series. The main differences thus observed between the two pyrolysates are now discussed.

The *n*-alkylbenzothiophenes and *n*-alkylmethylbenzothiophenes exhibit large changes in distribution between the two procedures (Fig. 10). For the "indirect" experiment, long alkyl chains (up to C_{14}) are observed whereas only short chain compounds ($<C_4$) are formed upon "direct" pyrolysis. Such a difference may reflect the occurrence, in the unheated material, of *n*-alkylbenzothiophene moieties whose chain would be linked to the macromolecular structure via several sulfide bridges, as observed by Sinninghe Damsté et al. (1990, 1998) for various kerogens. Pre-heating at 300 °C would result in the cleavage of some of these sulfide linkages, thus promoting the subsequent release of compounds with relatively long alkyl chains. In contrast "direct" heating at 400 °C would favour β cleavage and, to a lesser extent, γ and δ cleavages, hence the release of alkylbenzothiophenes with very short chains. Similarly, a sharp lowering is noted from C_{10} for the distribution of the 2-*n*-alkyl-5′-methyl-2′,5-bithiophenes in the case of the "direct" pyrolysis (Fig. 11), instead of a regular decrease in intensity. Accordingly, for this series of bithiophenes

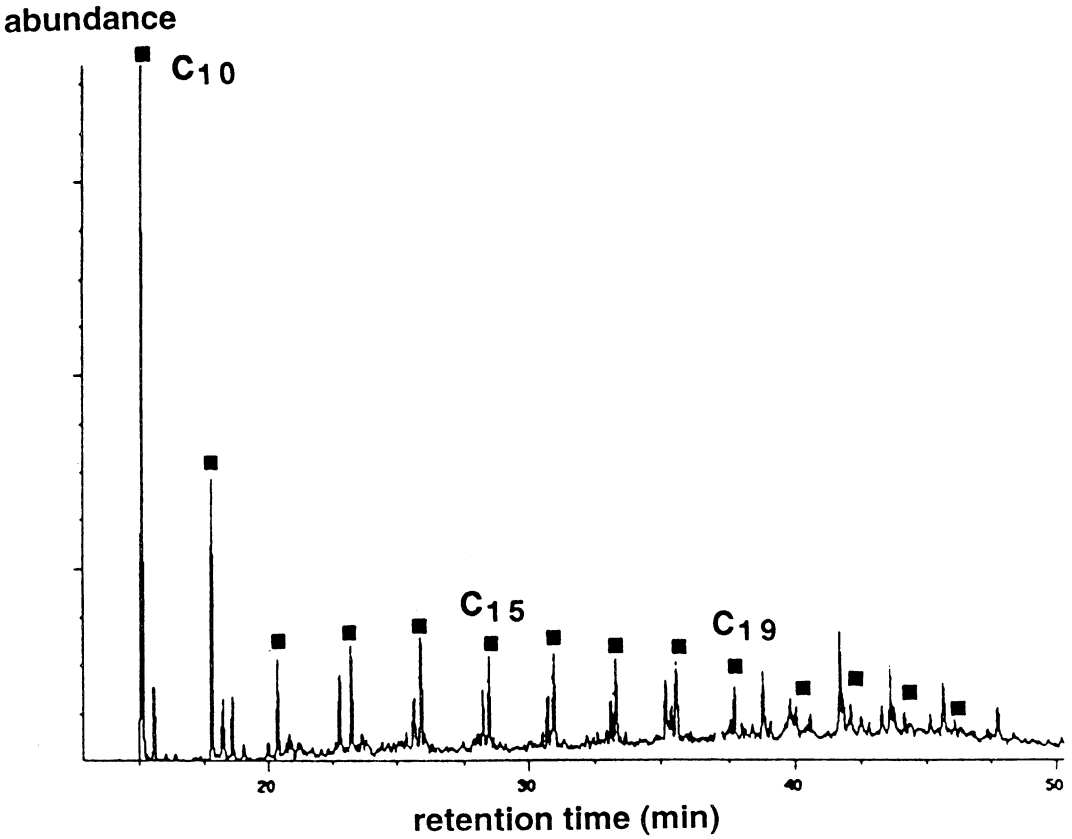

Fig. 11. Distributions of the 2-*n*-alkyl-5′-methyl-2′,5-bithiophenes formed via "direct" pyrolysis at 400 °C of TM9sa kerogen (mass chromatogram *m*/*z* 193).

Table 3
Comparison of the bulk quantitative features of the "direct" and "indirect" pyrolysis of TM9sa kerogen

	Total loss[a]	Trapped/volatile[c]	Fractionation of crude pyrolysate[d]				Pyrolysis residue[e]	
			Heptane	Toluene	MeOH	Retained	H/C	S org/C
"Direct"	90.2	1.14	27	39.5	15	18.5	0.75	0.07
"Indirect"	85.4[b]	1.77	10.5	27	8	54.5	0.75	0.10

[a] Total amount of pyrolysis products swept away by the He flow (wt.% of TM9sa kerogen). The medium to low volatility pyrolysis products (e.g. C_9+ compounds for *n*-alkanes) are trapped in cold chloroform (crude pyrolysate).

[b] Summed loss from pre-heating at 300 °C and subsequent "indirect" pyrolysis at 400 °C (after Mongenot et al., 1999).

[c] Relative amounts (ratio) of trapped pyrolysis products and of high volatility pyrolysis products (not trapped in cold chloroform). The values show that the pyrolysates are not dominated by highly volatile low molecular weight compounds, but by non GC-amenable components with relatively high molecular weights (Mongenot et al., 1999).

[d] See note (b) Table 1. Relative abundances (wt.% of crude pyrolysate) of the fractions (eluted with heptane, toluene and methanol, respectively) recovered by CC fractionation of the pyrolysate and of the high molecular weight products retained on the column. The latter value was calculated by difference.

[e] Atomic ratios, obtained by elemental analysis, of the insoluble pyrolysis residues (initial H/C and S org/C ratios in the unheated kerogen: 1.44 and 0.089, respectively).

as well, "direct" pyrolysis appears to promote β cleavage instead of cleavage of the sulfide bridges.

A few series of OSCs, such as the 2-*n*-alkenyl-5-methylthiophenes, previously identified in the heptane-eluted pyrolysis products from the "indirect" pyrolysis (Mongenot et al., 1999), are not produced in significant amounts in the "direct" experiment. The changes in some sulfur functions and/or in their environment is also reflected in the presence of new OSC in the "direct" pyrolysate, including dimethyldibenzothiophene isomers and C_{13}–C_{19} *n*-alkenylmethylbithiophenes. Also, the C_{16} and C_{18} *n*-alkan-1-ols and the C_{18} *n*-alkenol that dominate the individual peaks in the GC trace of the methanol-eluted non-acid fraction from the "indirect" pyrolysis (Mongenot et al., 1999) are no longer detected in the "direct" pyrolysate. Thus, some oxygen-containing groups are also modified by pre-heating at 300 °C.

Differences between the two methods also appeared following desulfurization and hydrogenation of the toluene-eluted fraction, the methanol-eluted non-acid fraction and the total pyrolysate. Desulfurization by Raney Ni is commonly used in studies concerned with sulfur-rich kerogens. This reaction provides information on the skeleton of the alkyl chains building up the macromolecular network through the cleavage of sulfide bridges and of sulfur-containing heterocycles. Desulfurization following "indirect" pyrolyses showed the abundant presence of sulfur-rich molecular aggregates in this pyrolysate (Mongenot et al., 1999). All of these aggregates are based on intermolecularly sulfur-bound *n*-alkyl chains with a typical distribution, i.e., C_{14} to C_{24}, marked by an even-over-odd predominance, and a sharp maximum at C_{18}. XANES spectroscopy provided further information on these aggregates, showing the lack of significant amounts of di(poly)sulfides in both pyrolysates (Table 1). This reflects the high sensitivity of di(poly)sulfide bridges to thermal stress, due to the easy cleavage of S–S bonds. Accordingly, the chains in the molecular aggregates are not cross-linked by di(poly) sulfide bridges but by monosulfide bridges. Sulfur in these aggregates generated upon "direct", and "indirect" pyrolyses is thus located in thiophenic structures (major form according to XANES results) and in sulfide linkages (Table 2). These two forms reflect the diagenetic incorporation of sulfur into lipids via intra- and intermolecular processes, respectively, that took place during the formation of TM9sa kerogen.

The aggregates generated from TM9sa kerogen under "indirect" conditions probably exhibit a large range of molecular weight (MW) (Mongenot et al., 1999). These aggregates correspond, in decreasing MW order, to (i) the components retained on the column during CC fractionation of the pyrolysate, which account for ca. 50 wt.% of the total "indirect" pyrolysate, (ii) the methanol-eluted non-GC-amenable compounds and (iii) the methanol-eluted GC-amenable compounds which contribute to the large hump observed in the GC trace of the methanol eluate. The MW of all these compounds, including the non-eluted aggregates, is low enough to allow them to be swept by the helium flow and dissolve in organic solvents. No molecular aggregates were observed in the toluene-eluted fraction for the "indirect" experiment. In fact, desulfurization of this fraction resulted in the formation of *n*-alkanes with a markedly different distribution (C_9–C_{31}, no even-over-odd predominance, no sharp maximum at C_{18}, regular decrease in intensity from C_{16}–C_{31}). These hydrocarbons originate from the low MW OSC abundantly occurring in the toluene-eluted fraction and directly identified via GC/MS analysis.

The distribution of the *n*-alkanes formed via desulfurization and hydrogenation of the toluene-eluted fraction from the "direct" pyrolysate is shown in Fig. 12. This distribution appears markedly different when compared to that from "indirect" pyrolysis. In contrast, it is similar, with a marked even-over-odd predominance in the C_{14}–C_{24} range, to the one observed for the desulfurization of the above mentioned sulfur-rich molecular aggregates (Mongenot et al., 1999). However, these aggregates generated by "direct" heating at 400 °C probably exhibit lower MW when compared to those occurring in the "indirect" pyrolysate, which explains their elution with toluene in the present case. Molecular aggregates also occur in the methanol-eluted non-acid fraction of the "direct" pyrolysate, as under "indirect" conditions. The high MW aggregates, not eluted from the chromatographic column, are much less abundant in the case of the "direct" pyrolysis (Table 3). Such a difference, added to the presence of "low MW" aggregates in the toluene-eluted fraction illustrates the higher efficiency of the latter pyrolysis for the thermal cracking of the macromolecular structure of TM9sa kerogen. This higher efficiency is reflected by a general shift of MW distribution to relatively lower values for the molecular aggregates formed via "direct" pyrolysis.

Another important difference between the "direct" and "indirect" experiments concerns the much lower efficiency of the desulfurization of the molecular aggregates generated under the former conditions, except for the "low MW" (toluene-eluted) fraction. Thus, a large hump is still observed after desulfurization of the methanol-eluted non-acid fraction, along with a very low production of hydrocarbons following desulfurization. These major differences were ascertained via parallel desulfurizations, using the same batch of catalyst, on the "direct" and "indirect" fractions. Moreover, no increase in efficiency was noted when the former fraction was submitted to a second desulfurization, thus indicating that catalyst poisoning was not important. Such a difference in efficiency also clearly appeared upon desulfurization of the crude pyrolysates. Three sources can be a priori implicated for the hydrocarbons of the desulfurized pyrolysate: (i) pre-existing compounds, i.e. hydrocarbons occurring as such in the untreated pyrolysate, (ii) desulfurization of low MW OSC and (iii) desulfurization of molecular aggregates. The latter

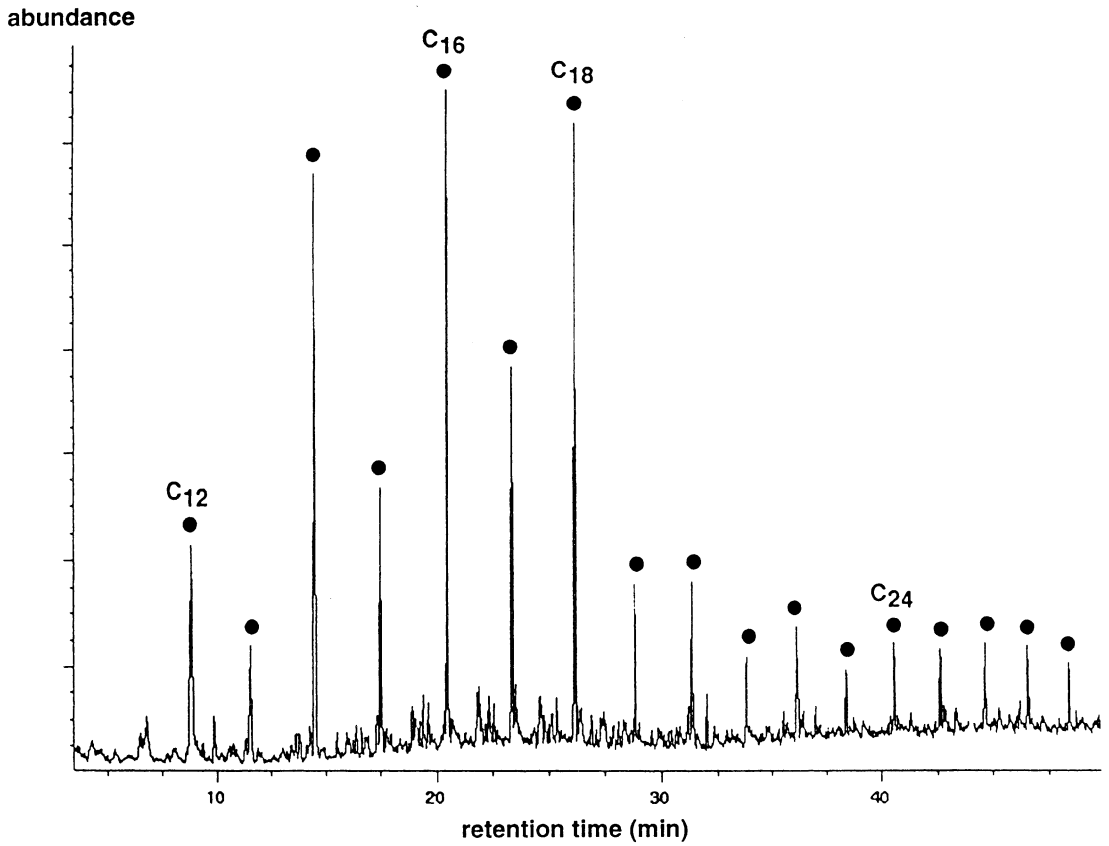

Fig. 12. Distribution of the *n*-alkanes (mass chromatogram *m*/*z* 57) obtained after desulfurization using Raney Ni and hydrogenation of the toluene-eluted fraction from "direct" pyrolysis at 400 °C of TM9sa kerogen.

source sharply dominates in the case of the "indirect" pyrolysis (Mongenot et al., 1999). In contrast, the distribution of the *n*-alkanes obtained from the "direct" pyrolysate (C_{12}–C_{33}, no even-over-odd predominance, no sharp maximum at C_{18}, regular decrease in intensity from C_{16} to C_{33}, Fig. 13) is consistent with a major contribution from pre-existing hydrocarbons and desulfurization products of low MW OSC whereas the *n*-alkanes derived from molecular aggregates did not afford a large contribution. Poor efficiency was previously noted for desulfurization of various rock extracts and kerogen pyrolysis products (e.g. van Kaam-Peters et al., 1998). Such a feature probably reflects steric protection of sulfur-containing functions within highly cross-linked macromolecular structures. Steric protection is well documented in the case of algaenans and derived kerogens (e.g. Largeau et al., 1986). Indeed, the ester groups protected within such bio- and geomacromolecules are not cleaved by drastic base and acid treatments and can also survive diagenetic degradation. It

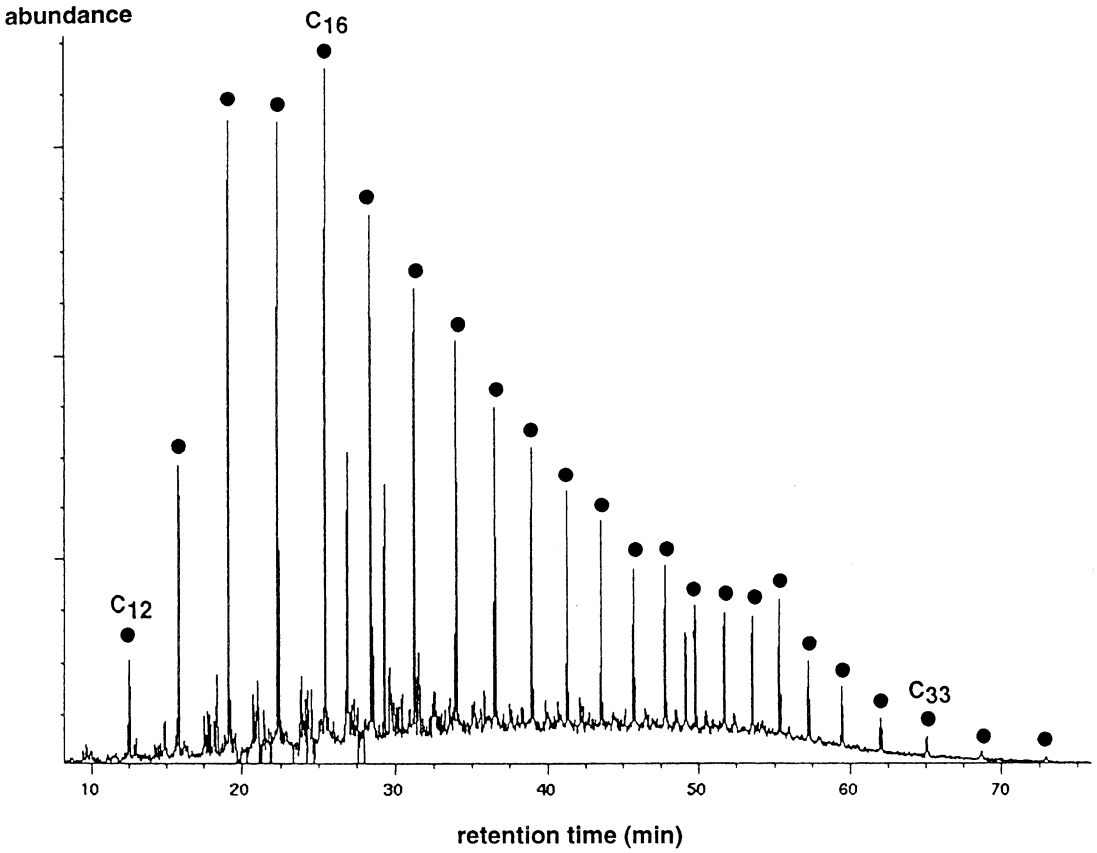

Fig. 13. Distribution of the *n*-alkanes (mass chromatogram *m*/*z* 57) obtained after desulfurization using Raney Ni and hydrogenation of the total pyrolysate from "direct" pyrolysis at 400 °C of TM9sa kerogen.

Table 4
Comparison between "indirect" and "direct" pyrolyses at 400 °C; consequences of the changes in the chemical structure of TM9sa kerogen induced by pre-heating at 300 °C for the "indirect" pyrolysis

(1) Somewhat lower production of pyrolysis products (volatile + trapped)
(2) Higher trapped/volatile ratio
(3) Shift of MW of molecular aggregates to higher values (larger production of high MW, non-eluted aggregates; lack of "low MW", toluene-eluted, aggregates)
(4) Less efficient release of sulfur-containing species
(5) Longer alkyl chains in some series of OSC formed by pyrolysis
(6) Lower degree of cross-linking in molecular aggregates (reflected by much higher efficiency of desulfurization)

seems therefore that sterically protected sulfur-containing groups abundantly occur in the molecular aggregates generated through "direct" pyrolysis of TM9sa kerogen but not (or to a markedly lower extent) in the "indirect" pyrolysate. As already stressed, pre-heating at 300 °C results in changes in some sulfur functions of TM9sa kerogen and/or in their environment and is also probably associated with the cleavage of some sulfide linkages. Such cleavages would not result in the formation of high MW units, volatile enough to be swept away by the helium flow at 300 °C, but they would influence the structure of the sulfur-rich aggregates released by subsequent, "indirect", pyrolysis at 400 °C. As a result, these aggregates would be more sensitive to desulfurization than those formed through "direct" heating, due to a lower degree of cross-linking and hence to a lower degree of steric protection of sulfide linkages between the alkyl chains.

This comparative study therefore has shown important quantitative and qualitative differences, which are summarized in Table 4, between "direct" and "indirect" pyrolysis. The latter is substantially influenced by the changes that occur in the structure of TM9sa kerogen, especially in the sulfur functions, during pre-heating at 300 °C. These changes are likely related to the occurrence of some aromatization reactions, revealed by FTIR, and to the cleavage of some sulfide linkages. When bulk features are compared, the "indirect" pyrolysis appears relatively less efficient for the thermal cracking of the macromolecular structure of the kerogen (1–4). Nevertheless, more detailed information can be obtained on the structure of TM9sa kerogen via "indirect pyrolysis" (5, 6), especially through the release of alkyl chains from molecular aggregates by desulfurization.

4. Conclusions

The main conclusions of this study carried out via (i) a combination of sulfur K- and L-edge XANES spectroscopy and pyrolysis and (ii) comparison between "direct" and "indirect" pyrolyses, are as follows:

- Sulfur speciation is similar in the unheated kerogens from the five facies recognized in the Orbagnoux deposit. All these samples contain thiophenes as major species and disulfides, alkyl sulfides and thiols in smaller proportion. Some oxidized species probably occur in low amounts. The observation of thiophene predominance is important as previous spectroscopic and pyrolytic studies could not provide information on the presence of thiophenic units in Orbagnoux kerogens.
- The pre-heating treatment induces some decrease in the disulfide content. The contribution of the most oxidized species tends to increase but remains minor.
- Pyrolysis at 400 °C completely removes the disulfide, alkyl sulfide and thiol species in the insoluble residue. The major species remaining corresponds to thiophenes, which are probably included in condensed structures. The contribution of oxidized species increases, especially at the surface of the grains. The latter feature probably reflects oxidation during sample handling and it is more marked for the "indirect" pyrolysis.
- The pyrolysis effluents contain thiophenes as major sulfur species, plus some alkyl sulfides and/or thiols and oxidized moieties. No significant difference in sulfur speciation was observed by S K-and L-edge XANES spectroscopy between the effluents from "direct" and "indirect" pyrolyses. However, XANES spectroscopy provided further information on the chemical structure of the aggregates abundantly produced upon pyrolysis of TM9sa kerogen at 400 °C. It appeared that the alkyl chains that build up such aggregates are not cross-linked by di(poly)sulfide bridges but by monosulfide bridges. Sulfur in these aggregates is located in thiophenic structures (major form) and in such sulfide linkages. These two forms reflect the diagenetic incorporation of sulfur in lipids via intra- and intermolecular processes, respectively, that took place during the formation of TM9sa kerogen.
- Important quantitative and qualitative differences are observed between "direct" and "indirect" pyrolyses of TM9sa kerogen at 400 °C. Pre-heating at 300 °C in the "indirect" experiment results in some changes in the chemical structure of the kerogen, due to aromatization and cleavage of some sulfide linkages. Such changes substantially influence the subsequent "indirect" pyrolysis at 400 °C. When bulk features are compared, "indirect" pyrolysis appears less efficient for the thermal cracking of the macromolecular structure of the kerogen, as indicated by a slightly lower production of total (trapped + volatile) pyrolysis products, a lower relative abundance of volatile compounds, a shift in MW of molecular aggregates to higher values, and a less efficient release of sulfur-containing functions. Nevertheless, more detailed information can be obtained on the structure of TM9sa kerogen via this method owing to (i) the release of some series of OSC where longer alkyl chains are retained and (ii) much easier desulfurization of molecular aggregates, probably due to a lower degree of cross-linking.

- Comparison of the contribution of non-thiophenic sulfur as reflected by H_2S production with the contribution determined via XANES spectroscopy showed the occurrence of substantial aromatization of the non-thiophenic sulphur of the kerogen into thiophenic structures upon pyrolyses. This aromatization is somewhat more pronounnced in the case of the "indirect" experiment.

Acknowledgements

This study was financed by the National Research Council of Canada, the Natural Science and Engineering Research Council of Canada, and Elf Exploration Production. G.S. would like to acknowledge Elf Exploration Production for providing fellowship. We are grateful to Dr. Kim Tan from CSRF and the staff of the Synchrotron Radiation Center (SRC), University of Wisconsin, Madison, for their technical support, and National Science Foundation (NSF) for supporting the SRC under Award # DMR-(95–31009). Yves Pouet is acknowledged for technical support for GC/MS analyses.

Associate Editor—**C.E. Snape**

References

Bernier, P., 1984. Les formations carbonatées du Kimméridgien et du Portlandien dans le Jura méridional. Stratigraphie, micropaléontologie et sédimentologie. Document du Laboratoire de Géologie de la Faculté des Sciences de Lyon 92.

Bernier, P., Courtinat, B., 1979. Le microplancton (Leiosphaeridae) et la matière organique des calcaires d'arrière-récif du Kimméridgien supérieur dans le Jura méridional. Systématique, conditions de génèse et d'environnement. Document du Laboratoire de Géologie de la Faculté des Sciences de Lyon 75, 95–117.

Brown, J.R., Kasrai, M., Bancroft, G.M., Tan, K.H., Chen, J.M., 1992. Direct identification of organic sulfur species in Rasa Coal from sulfur L-edge X-ray absorption near-edge spectra. Fuel 71, 649–653.

Brown, S.D., Sirkecioglu, O., Snape, C.E., Eglinton, T.I., 1997. Speciation of the organic sulphur forms in a recent sediment and type I and II-S kerogens by high pressure temperature programmed reduction. Energy and Fuels 11, 532–538.

Brown, S.D., Chiavari, G., Ediger, V., Fabbri, D., Gaines, A.F., Galletti, G., Kariyigit, A.I., Love, G.D., Snape, C.E., Sirkecioglu, O., Toprak, S., 2000. Black Sea sapropels: relationship to kerogens and fossil fuel precursors. Fuel 79, 1725–1742.

Calkins, W.H., 1987. Investigation of organic sulfur-containing structures in coal by flash pyrolysis experiments. Energy and Fuels 1, 59–64.

Chauvistré, R., Hormes, J., Hartmann, E., Etzenbach, N., Hosch, R., Hahn, J., 1997. Sulfur K-shell photoabsorption spectroscopy of the sulfanes R-S_n-R, n = 2–4. Chemical Physics 223, 293–302.

Cohen, Y., Krein, E.B., Aizenshtat, Z., 1995. Structural reconstruction of sulfur-rich kerogens via pyrolysis of natural and synthetic polymers. In: Grimalt, J.O., Dorronsoro, C. (Eds.), Organic Geochemistry: Developments and Applications to Energy, Climate, Environment and Human History. A. I. G. O. A, Donostia-San Sebastian, pp. 936–939.

Czarnetzki, B.M., 1986. Effect of shale oils (ichthyols) on the secretion of chemolactic leukotrienes from human leucocytes and on leucocyte migration. J. Invest. Dermatol. 87, 694–697.

Durand, B., Monin, J.C., 1980. Elemental analysis of kerogens (C, H, O, N, S, Fe). In: Durand, B. (Ed.), Kerogen. Editions Technip, Paris, pp. 113–141.

Durand, B., Nicaise, G., 1980. Procedures for kerogen isolations. In: Durand, B. (Ed.), Kerogen. Technip, Paris, pp. 35–53.

Eglinton, T.I., Sinninghe Damsté, J.S., Kohnen, M.E.L., de Leeuw, J., Larter, S.R., Patience, R., 1990. Analysis of maturity-related changes in organic sulfur composition of kerogens by flash pyrolysis-gas chromatography. In: Orr, W.L., White, C.M. (Eds.), Geochemistry of Sulfur in Fossil Fuels. ACS Symposium Series 429. American Chemical Society, Washington, DC, pp. 529–565.

Eglinton, T.I., Sinninghe Damsté, J.S., Pool, W., de Leeuw, J., Eijkel, G., Boon, J.J., 1992. Organic sulfur in macromolecular sedimentary organic matter—II. Analysis of distribution of organic sulfur-containing pyrolysis products using multivariate techniques. Geochimica et Cosmochimica Acta 56, 1545–1560.

Eglinton, T.I., Irvine, J.E., Vairavamurthy, A., Zhou, W., Manowitz, B., 1994. Formation and diagenesis of macromolecular organic sulfur in Peru margin sediments. Organic Geochemistry 22, 781–799.

George, G.N., Gorbaty, M.L., 1989. Sulfur K-edge absorption spectroscopy of petroleum asphaltenes and model compounds. Journal of the American Chemical Society 111, 3182–3186.

George, G.N., Gorbaty, M.L., Kelemen, S.R., 1990. Sulfur K-edge absorption spectroscopy of petroleum asphaltenes and model compounds. In: Orr, W.L., White, C.M. (Eds.), Geochemistry of Sulfur in Fossil Fuels. ACS Symposium Series 429. American Chemical Society, Washington, DC, pp. 220–230.

Gillaizeau, B., Behar, F., Derenne, S., Largeau, C., 1997. Nitrogen fate during laboratory maturation of a type I kerogen (Oligocene, Turkey) and related algaenan: nitrogen mass balances and timing of N2 production versus other gases. Energy and Fuels 11, 1237–1249.

Gorbaty, M.L., George, G.N., Kelemen, S.R., 1990. Direct determination and quantification of sulfur forms in heavy petroleum and coals. 2. The sulfur K-edge absorption spectroscopy approach. Fuel 69, 945–949.

Gorin, G., Gülaçar, F., Cornioley, Y., 1989. Organic geochemistry, palynofacies and palaeoenvironment of Upper Kimmeridgian and Lower Tertiary organic-rich samples in the southern Jura (Ain, France) and subalpine massifs (Haute-Savoie, France). Eclogae Geologicae Helvetica 82, 491–515.

Green, J.B., Yu, S.K.-T., Pearson, C.D., Reynolds, J.W., 1993. Analysis of sulfur type compounds in asphalts. Energy and Fuels 7, 119–126.

Gubler, Y., Louis, M., 1956. Etudes d'un certain milieu du Kimméridgien bitumineux de l'Est de la France. Revue de l'Institut Français du Pétrole 11, 1536–1543.

Huffman, G.P., Huggins, F.E., Mitra, S.N., Pugmire, R.J., Davis, B., Lytle, F.W., Greegor, R.B., 1989. Investigation of the molecular structure of organic sulfur in coals by XAFS spectroscopy. Energy and Fuels 3, 200–205.

Huffman, G.P., Mitra, S.N., Huggins, F.E., Shah, N., Vaidya, S., Lu, F., 1991. Quantitative analysis of all major forms of sulfur in coals by X-ray absorption fine structure spectroscopy. Energy and Fuels 5, 574–581.

Kasrai, M., Bancroft, G.M., Brunner, R.W., Jonasson, R.G., Brown, J.R., Tan, K.H., Feng, X., 1994. Sulfur speciation in bitumens and asphaltenes by X-ray absorption fine structure spectroscopy. Geochimica et Cosmochimica Acta 58, 2865–2872.

Kasrai, M., Brown, J.R., Bancroft, G.M., Yin, Z., Tan, K.H., 1996a. Sulfur characterization in coal from X-ray absorption near edge spectroscopy. International Coal Geology 32, 107–135.

Kasrai, M., Lennard, W.N., Brunner, R.W., Bancroft, G.M., Bardwell, J.A., Tan, K.H., 1996. Sampling depth of total electron and fluorescence measurements in Si L- and K-edge absorption spectroscopy. Applied Surface Science 99, 303–312.

Kelemen, S.R., Gorbaty, M.L., George, G.N., Kwiatek, P.J., Sansone, M., 1991. Thermal reactivity of sulfur forms in coal. Fuel 70, 396–402.

Kelemen, S.R., Vaughn, S.N., Gorbaty, M.L., Kwiatek, P.J., 1993. Transformation kinetics of organic sulfur forms in Argonne Premium coals during pyrolysis. Fuel 72, 646–653.

Koch, J., Moser, R., Demel, J., 1985. Analyse des Ammoniumbituminosulfonates ICHTHYOL. Arch. Pharm. 318, 198–206.

Koopmans, M.P., Sinninghe Damsté, J.S., Lewan, M.D., de Leeuw, J.W., 1995. Thermal stability of thiophenes biomarkers as studied by hydrous pyrolysis. Organic Geochemistry 23, 583–596.

Koopmans, M.P., Köster, J., van Kaam-Peters, H.M.E., Kenig, F., Schouten, S., Hartgers, W.A., de Leeuw, J.W., Sinninghe Damsté, J.S., 1996. Diagenetic and catagenetic products of isorenieratene: molecular indicators for photic zone anoxia. Geochimica et Cosmochimica Acta 60, 4467–4496.

Krein, E.B., Aizenshtat, Z., 1994. The formation of isoprenoid sulfur compounds during diagenesis: simulated sulfur incorporation and thermal transformation. Organic Geochemistry 21, 1015–1025.

Largeau, C., Derenne, S., Casadevall, E., Kadouri, A., Sellier, N., 1986. Pyrolysis of immature Torbanite and of the resistant biopolymer (PRB A) isolated from extant alga *Botryococcus braunii*. Mechanism of formation and structure of Torbanite. Organic Geochemistry 10, 1023–1032.

Mitchell, S.C., Snape, C.E., Garcia, R., Ismail, K., Bartle, K.D., 1994. Determination of organic sulfur forms in some coals and kerogens by high pressure temperature-programmed reduction. Fuel 73, 1159–1166.

Mongenot, T., Boussafir, M., Derenne, S., Lallier-Vergès, E., Largeau, C., Tribovillard, N.P., 1997. Sulfur-rich organic matter from bituminous laminites of Orbagnoux (France, Upper Kimmeridgian). The role of early vulcanization. Bulletin de la Société Géologique de France 168, 331–341.

Mongenot, T., Derenne, S., Largeau, C., Tribovillard, N.P., Lallier-Vergès, E., Dessort, D., Connan, J., 1999. Spectroscopic, kinetic and pyrolytic studies of kerogen from the dark parallel laminae facies of the sulfur-rich Orbagnoux deposit (Upper Kimmeridgian, Jura). Organic Geochemistry 30, 39–56.

Mongenot, T., Tribovillard, N.P., Arbey, F., Lallier-Vergès, E., Derenne, S., Largeau, C., Pichon, R., Dessort, D., Connan, J., 2000. Comparative studies of high resolution samples from the Orbagnoux deposit (Upper Kimmeridgian, Jura) via petrographic and bulk geochemical methods. Extent and origin of interfacies and intrafacies variations. Bulletin de la Société Géologique de France 171, 23–36.

Nelson, B.C., Eglinton, T.I., Seewald, J.S., Vairavamurthy, M.A., Miknis, F.P., 1995. Transformation in organic sulfur speciation during maturation of the Monterey shale: constraints from laboratory experiments. In: Vairavamurthy, M.A., Schoonen, M.A.A. (Eds.), Geochemical Transformation of Sedimentary Sulfur. ACS Symposium Series 612. American Chemical Society, Washington, DC, pp. 138–166.

Riboulleau, A., Derenne, S., Sarret, G., Largeau, C., Baudin, F., Connan, J., 2000. Pyrolytic and spectroscopic study of a sulphur-rich kerogen from the "Kashpir oil shales" (Upper Jurassic, Russian Platform). Organic Geochemistry Washington, DC 31, 1641–1661.

Rouxhet, P.G., Robin, P.L., Nicaise, G., 1980. Characterization of kerogens and of their evolution by infrared spectroscopy. In: Durand, B. (Ed.), Kerogen. Editions Technip, Paris, pp. 163–190.

Sarret, G., Connan, J., Kasrai, M., Eybert-Bérard, L., Bancroft, G.M., 1999a. Chemical form of sulfur in recent geological and archeological asphaltenes from Middle East, France and Spain determined by sulfur K- and L-edge XANES spectroscopy. Geochimica et Cosmochimica Acta 63, 3767–3779.

Sarret, G., Connan, J., Kasrai, M., Eybert-Bérard, L., Bancroft, G.M., 1999. Characterization of sulfur in asphaltenes by sulfur K- and L-edge XANES spectroscopy. Journal of Synchrotron Radiation 6, 670–672.

Schmid, J.C., 1986. Marqueurs Biologiques Soufrés dans les Pétroles. PhD Thesis, University Louis Pasteur, Strasbourg.

Schouten, S., Sinninghe Damsté, J.S., de Leeuw, J.W., 1995. The occurrence and distribution of low-molecular-weight sulfoxides in polar fractions of sediment extracts and petroleum. Organic Geochemistry 23, 129–138.

Sinninghe Damsté, J.S., ten Haven, H.L., de Leeuw, J.W., Schenck, P.A., 1986. Organic geochemical studies of a Messinian evaporitic basin, northern Apennines (Italy). II Isoprenoid and n-alkyl thiophenes and thiolanes. In: Leythaeuser, D., Rullkötter, J. (Eds.), Advances in Organic Geochemistry 1985. Pergamon Press, Oxford Organic Geochemistry, pp. 791–805.

Sinninghe Damsté, J.S., Rijpstra, W.I.C., de Leeuw, J.W., Schenck, P.A., 1988a. Origin of organic sulfur compounds and sulfur-containing high molecular weight substances sediments and immature crude oils. In: Mattavelli, L., Novelli, L., (Eds.), Advances in Organic Geochemistry 1987. Pergamon Press, Oxford. Organic Geochemistry 13, 593–606.

Sinninghe Damsté, J.S., Kock-van Dalen, A.C., de Leeuw, J.W., Schenck, P.A., 1988. The identification of homologous series of alkylated thiophenes, thiolanes, thianes and benzothiophenes present in pyrolysates of sulfur-rich kerogen. Journal of Chromatography 435, 435–452.

Sinninghe Damsté, J.S., de Leeuw, J., 1990. Organically-bound sulfur in the geosphere: state of the art and future research. Organic Geochemistry 16, 1077–1101.

Sinninghe Damsté, J.S., Eglinton, T.I., Rijpstra, W.I.C., de Leeuw, J.W., 1990. Charaterization of organically bound sulfur in high-molecular-weight, sedimentary organic matter using flash pyrolysis and Raney Ni desulfurization. In: Orr, W.L., White, C.M. (Eds.), Geochemistry of Sulfur in Fossil Fuels. ACSSS, 429. American Chemical Society, Washington, DC, pp. 486–528.

Sinninghe Damsté, J.S., Kohnen, M.E., Horsfield, B., 1998. Origin of low-molecular-weight alkylthiophenes in pyrolysates of sulfur-rich kerogens as revealed by micro-scale sealed vessel pyrolysis. Organic Geochemistry 29, 1891–1904.

Spiro, C.L., Wong, J., Lytle, F.W., Greegor, R.B., Maylotte, D.H., Lamson, S.H., 1984. X-ray absorption spectroscopic investigation of sulfur sites in coals: organic sulfur identification. Science 226, 48–50.

Tomic, J., Behar, F., Vandenbroucke, M., Kagi, I., 1995. Artificial maturation of Monterey kerogen (type II-S) in a closed system and comparison with type II kerogen: implications on the fate of sulfur. Organic Geochemistry 23, 47–660.

Tribovillard, N.P., Gorin, G., Hopfgartner, G., Manivit, H., Bernier, P., 1991. Conditions de dépôts et matière organique en milieu lagunaire d'âge Kimméridgien du Jura méridional français (résultats préliminaires). Eclogae Geologicae Helvetia 84, 441–461.

Tribovillard, N.P., Gorin, G., Belin, S., Hopfgartner, G., Pichon, R., 1992. Organic-rich biolaminated facies from a Kimmeridgian lagoonal environment in the French Southern Jura mountains—a way of estimating accumulation rate variations. Palaeogeography Palaeoclimatology Palaeoecology 99, 163–177.

Vairavamurthy, A., Zhou, W., Eglinton, T.I., Manowitz, B., 1994. Sulfonates: a novel class of organic sulfur compounds in marine sediments. Geochimica et Cosmochimica Acta 58, 4681–4687.

Vairavamurthy, M.A., Wang, S., Khandelwall, B., Manowitz, B., Ferdelman, T., Fossing, H., 1995. Sulfur transformation in early diagenetic sediments from the Bay of Conception, off Chile. In: Vairavamurthy, M.A., Schoonen, M.A.A. (Eds.), Geochemical Transformation of Sedimentary Sulfur. ACS Symposium Series 612. American Chemical Society, Washington, DC, pp. 38–58.

van Kaam-Peters, H.M.E., Köster, J., de Leeuw, J.W., Sinninghe Damsté, J.S., 1995. Occurrence of two novel benzothiophenes hopanoid families in sediments. Organic Geochemistry 23, 607–616.

van Kaam-Peters, H.M.E., Sinninghe Damsté, J.S., 1997. Characterization of an extremely organic sulfur-rich 150 Ma old carbonaceous rock: palaeoenvironmental implications. Organic Geochemistry 27, 371–397.

van Kaam-Peters, H.M.E., Rijpstra, W.I.C., de Leeuw, J.W., Sinninghe Damsté, J.S., 1998. A high resolution biomarker study of different lithofacies of organic sulfur-rich carbonate rocks of a Kimmeridgian lagoon (French southern Jura). Organic Geochemistry 28, 151–177.

Waldo, G.S., Carlson, R.M.K., Moldowan, J.M., Peters, K.E., Penner-Hahn, J.E., 1991. Sulfur speciation in heavy petroleum: information from X-ray absorption near-edge structure. Geochimica et Cosmochimica Acta 55, 801–814.

Waldo, G.S., Mullins, O., Penner-Hahn, J.E., Cramer, S.P., 1992. Sulfur speciation in heavy petroleum: determination of the chemical environment of sulfur in petroleum asphaltenes by X-ray absorption spectroscopy. Fuel 71, 53–57.